

Direct Estimation of Time Difference of Arrival from Compressive Sensing Measurements

Y.T. Chan¹, F. Chan¹, S. Rajan², B.H. Lee¹

¹ Dept. of Electrical and Computer Engineering, Royal Military College of Canada, Kingston, Ontario, Canada

² Defence Research and Development Canada, Ottawa, Ontario, Canada.

Abstract— In many applications such as localization, there is a need to determine the unknown time shift D between a signal, and its time shifted version. Aligning one against the other until the two match will find D . When working with compressive sensing (CS) measurements, only linearly transformed samples of the signal and its time-shifted version are available. These CS samples conceal the explicit time shift relationship between the signals, and D can no longer be found by a simple alignment of the CS measurements. As a result, estimation of the time-difference-of-arrival (TDOA) from CS measurements requires the restoration of the original signals. The nonlinear restoration can be time consuming, and may introduce large errors when noise is present. This paper provides an alternate TDOA estimator that avoids restoration. The key is in making additional measurements to preserve the time shift relationship of the signals. This requires a slight modification of the random modulator pre-integrator, as described in the paper, which also includes a simulation example.

Keywords—compressed sensing; TDOA estimation; random modulator pre-integrator.

I. INTRODUCTION

Passive localization of an emitter has applications in Wireless Sensor Networks [1], search and rescue operations [2] and target tracking [3]. Receivers at known but separate locations make measurements on a signal arriving from an emitter to determine its location. Typical measurements are, for example, angle-of-arrival, signal strength, time-of-arrival, and the most commonly used, time-difference-of-arrival (TDOA). The TDOA of a signal between two receivers, multiplied by the speed of a signal, gives the distance difference. The locus of points, which are at a fixed distance difference between two receivers is a hyperbola. The emitter lies on this locus. Hence for a two-dimensional localization, the TDOA from three or more receivers can generate hyperbolae whose intersection is the emitter location.

A standard TDOA estimator cross-correlates the output of two receivers [5]. The shift from the origin where the cross-correlation function peaks is the TDOA estimate. Let $s(t)$ and $s(t+D)$ be the output of two receivers. Their cross-correlation function peaks at a shift D , which is the TDOA.

Many new research areas arise with the advent of Compressive Sensing (CS): for example, how to estimate TDOA from CS measurements. These measurements are reduced dimension linear transformations of the time samples of the signals, resulting in underdetermined systems of

equations. They mask the time shift relationship between signals. To see this, let the $N \times 1$ vector samples of $s(t)$, from receiver 1 (R1) be

$$\mathbf{s} = [s(0) \dots s(N-1)]^T \quad (1)$$

and its time-shifted version $s(t+D)$ from receiver 2 (R2) be

$$\mathbf{s}_D = [s(D) \dots s(N-1+D)]^T \quad (2)$$

The sampling clocks of R1 and R2 are synchronized – a fundamental requirement in a TDOA system. The Nyquist sampling interval T_s to obtain (1) and (2) is taken to be $T_s \leq 1/(2B)$ with B being the maximum bandwidth of the two signals. Without loss of generality the sequel takes $T_s=1$. Also, for illustration simplicity, D is assumed to be an integer, i.e., an integral multiple of the sampling interval. The CS measurement vector from R1 is

$$\mathbf{w} = \mathbf{A}\mathbf{s} \quad (3)$$

and from R2

$$\mathbf{w}_D = \mathbf{A}\mathbf{s}_D \quad (4)$$

where \mathbf{A} is a known $M \times N$ ($M < N$) measurement matrix. While the cross-correlation function of \mathbf{s} and \mathbf{s}_D have a peak at shift D from the origin, the same does not hold for \mathbf{w} and \mathbf{w}_D . The transformation by \mathbf{A} has masked the time shift relationship of \mathbf{s} and \mathbf{s}_D . Hence, it is necessary to first restore \mathbf{s} and \mathbf{s}_D , by l_1 minimization [6] for example, before TDOA estimation. This is the basis of the estimators in [7-11].

The restoration algorithms mostly are nonlinear and can be computationally expensive and subject to large errors if noise is present. This paper introduces a TDOA estimator that avoids restoration. The key is to make several CS measurements of time shifted versions of $s(t)$ and $s(t+D)$, and then estimate directly from the measurement vectors. Specifically, let the additional measurements from (3) and (4) be

$$\mathbf{w}^{(i)} = \mathbf{A}\mathbf{s}^{(i)} \quad (5)$$

and

$$\mathbf{w}_D^{(j)} = \mathbf{A}\mathbf{s}_D^{(j)} \quad (6)$$

where

$$\mathbf{s}^{(i)} = [s(i) \dots s(i+N-1)]^T \quad (7)$$

and

$$\mathbf{s}_D^{(j)} = [s(j+D) \dots s(j+D+N-1)]^T \quad (8)$$

for $i, j = 0, \dots, K-1$. Assume that $D \leq |D|_{\max}$, a maximum known *a priori*. This is not a restrictive assumption since

$|D|_{\max}$ serves only as a bound, which can be a loose bound. Choose $K \geq |D|_{\max}$ to ensure that there are i, j such that $i - j = D$. For example, if $D = 2$ and $K = 3$, then $\mathbf{w}^{(2)}$ and $\mathbf{w}_D^{(0)}$ will match perfectly.

It requires a slight modification of the CS signal acquisition procedure to obtain $\mathbf{w}^{(i)}$ and $\mathbf{w}_D^{(j)}$. In the rest of the paper, Section II describes the modification and the estimation of TDOA, directly from the CS measurements. Section III gives a simulation example, which experimentally checks the probability of making a correct estimation, against the theoretical prediction. Conclusions are in Section IV.

There are two novel contributions in this paper:

- (i) Estimation of TDOA from CS measurements without restoration, and
- (ii) Provision of CS measurements that preserve the time shift relationship between the two signals.

II. DIRECT TDOA ESTIMATION

A. Acquisition of CS measurements

The Random Modulator Pre-Integrator (RMPI) [12] can acquire the CS measurements of a signal at below the Nyquist-rate. As shown in [12], an RMPI has M channels. Each channel multiplies the analog input with a pseudo random bit sequence (PRBS), whose bit values are ± 1 , integrates the products, and then samples the output to give one CS measurement. The PRBS of the M channels are uncorrelated with each other. With M channels, the RMPI outputs an $M \times 1$ vector of CS measurements.

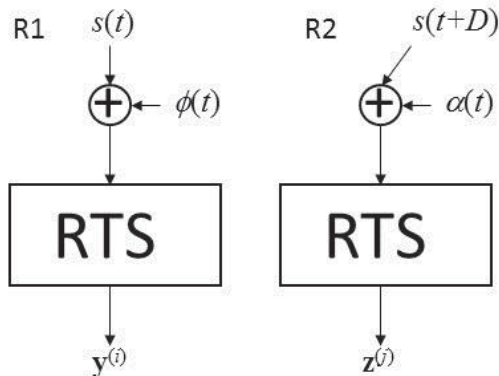


Fig. 1. Obtaining CS measurement vector.

Consider now a modification of the RMPI, called RMPI with time shift (RTS), with the purpose of acquiring CS measurements for direct TDOA estimation. In Fig. 1, arriving at R1 is the emitter signal $s(t)$ plus noise $\phi(t)$, and at R2, $s(t+D)$ plus noise $\alpha(t)$. The TDOA, D , can be a positive or negative number, whose value is dependent on the relative locations of the emitter and the receivers. The RTS output from R1 contain K vectors of $\mathbf{y}^{(i)}$, $i = 0, \dots, K-1$. Similarly from R2, the output are $\mathbf{z}^{(j)}$, $j = 0, \dots, K-1$. Each $\mathbf{y}^{(i)}$ is a CS measurement vector ($M \times 1$) of N samples of $s(t) + \phi(t)$. Let $\mathbf{s}^{(i)}$ be given by (7), and

$$\boldsymbol{\phi}^{(i)} = [\phi(i) \dots \phi(N-i+1)]^T \quad (9)$$

be the samples of $\phi(t)$.

Then,

$$\mathbf{y}^{(i)} = \mathbf{A}\mathbf{s}^{(i)} + \mathbf{A}\boldsymbol{\phi}^{(i)}. \quad (10)$$

Similarly, from R2,

$$\mathbf{z}^{(j)} = \mathbf{A}\mathbf{s}_D^{(j)} + \mathbf{A}\boldsymbol{\alpha}^{(j)} \quad (11)$$

where $\mathbf{s}_D^{(j)}$ is given by (8) and

$$\boldsymbol{\alpha}^{(j)} = [\alpha(j+D) \dots \alpha(N-1+j+D)]^T \quad (12)$$

are the samples of $\alpha(t)$.

Next, Fig. 2 illustrates the measurement process of the RTS in R1, where there are K blocks in RTS. Each block contains an M channel RMPI. Consider for example the generation of the 7-th entry (channel 6) of $\mathbf{y}^{(3)}$ (Block 4). In channel 6, the sequence 000PRBS(6) multiplies the input. The three leading zeros delay PRBS(6) by 3 bits and equivalently, the input by 3 bits, before multiplication. This is one way, among possibly others, of obtaining a time-delayed version of the samples of $s(t)$ and $\phi(t)$. The PRBS sequences contain bit values ± 1 , and are different for each PRBS(m). Thus, the elements of the matrix \mathbf{A} are ± 1 , corresponding to the bit values of the PRBS. The same RTS structure holds for R2, except that the input is $s(t+D) + \alpha(t)$.

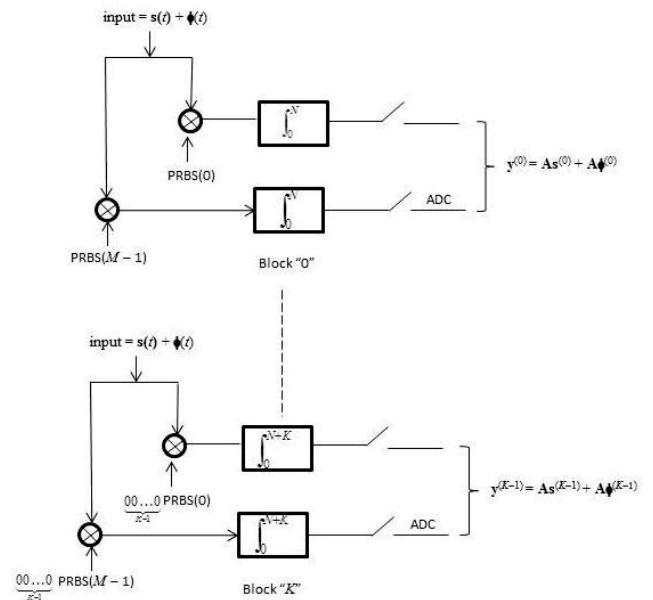


Fig. 2. RTS structure.

The number of channels M , and the length of PRBS are design parameters. The exact choice is application dependent and is a trade-off between measurement speed and hardware complexity. The RTS is able to acquire data at below the Nyquist rate, which may exceed the capabilities of the existing analog-to-digital converters, in terms of speed, power consumption and noise levels.

B. TDOA Estimation

If there is no noise, with the assumptions that $|D| \leq K$, there will be at least one perfect match between $\mathbf{y}^{(i)}$ and $\mathbf{z}^{(j)}$ in (11), with $i - j = D$. This fact leads to the TDOA estimate which computes the inner products

$$\Lambda_{i,j} = \langle \mathbf{y}^{(i)}, \mathbf{z}^{(j)} \rangle \quad (13)$$

for all $i, j = 0, \dots, K-1$, and selects the $\max(\Lambda_{i,j})$.

The estimate of the TDOA is

$$\hat{D} = i - j \quad (14)$$

corresponding to i, j in $\max(\Lambda_{i,j})$.

When noise is present, there is a finite probability of selecting a wrong maximum. To calculate the probability of obtaining a correct maximum, let the true $\max(\Lambda_{i,j})$ be Λ_* . Then, the probability of obtaining the correct TDOA estimate is

$$\text{Prob}(\ast) = \text{Prob}(\Lambda_* > \Lambda_{i,j}, \text{ for } \forall i - j \neq D) \quad (15)$$

Let a $K^2 - 1$ vector be

$$\boldsymbol{\gamma} = [\Lambda_{i,j} \dots]^T, \quad i - j \neq D \quad (16)$$

then (15) is given by

$$\text{Prob}(\ast) = \int_{\gamma=-\infty}^{\infty} \int_{\Lambda_*=\gamma}^{\infty} f(\Lambda_*, \boldsymbol{\gamma}) d\Lambda_* d\boldsymbol{\gamma}. \quad (17)$$

In (17), $f(\Lambda_*, \boldsymbol{\gamma})$ is the joint probability density function (pdf) of Λ_* and $\boldsymbol{\gamma}$, and with an abuse of notation, the lower limit $\Lambda_* = \gamma$ denotes Λ_* an element of $\boldsymbol{\gamma}$. The exact pdf is difficult to find. However, since N is large ($N=256$ for example), a Gaussian pdf assumption for $f(\Lambda_*, \boldsymbol{\gamma})$ is approximately valid by invoking the Central Limit theorem. Then

$$f(\Lambda_*, \boldsymbol{\gamma}) = \frac{\exp\left\{-\frac{1}{2}[\Lambda_* - \mu, \boldsymbol{\gamma}]^T \mathbf{R}^{-1} \begin{bmatrix} \Lambda_* - \mu \\ \boldsymbol{\gamma} \end{bmatrix}\right\}}{(2\pi)^{\frac{K}{2}} |\mathbf{R}|^{\frac{1}{2}}} \quad (18)$$

where \mathbf{R} is the co-variance matrix of Λ_* (of mean μ) and $\boldsymbol{\gamma}$ (of mean zero). The next Section contains an example that evaluates (17) and (18) to predict $\text{Prob}(\ast)$. The prediction matches closely the simulation results.

III. SIMULATION STUDIES

This section gives a simulation example of TDOA estimation, directly from the CS measurements. In (10) and (11), let $s(i)$, $\phi(i)$ and $\alpha(i)$ be zero mean white Gaussian random variables, with $\sigma_s^2 = E\{s^2(i)\}$, and $\sigma_\phi^2 = \sigma_\alpha^2 = E\{\phi^2(i)\} = E\{\alpha^2(i)\}$. The signal-to-noise ratio in dB is $\rho = 10 \log \sigma_s^2 / \sigma_\phi^2$. The 128×256 measurement matrix \mathbf{A} is the upper half of a 256×256 Hadamard matrix whose elements represent the PRBS bits.

The true D is equal to 3 and K is equal to 4, so that there are four $\mathbf{y}^{(i)}$ from (10) and four $\mathbf{z}^{(i)}$ from (11). For a given ρ , and 50,000 independent trials, the estimator at each trial chooses the largest (among the 16) $\Lambda_{i,j}$ as Λ_* , and gives the estimate as

$\hat{D} = i - j$. Recording the percentage of correct $\hat{D} = D$ then gives $\text{Prob}(\ast)$, the blue curve in Fig. 3.

For comparison, the theoretical $\text{Prob}(\ast)$ comes from the evaluation of (17). Now even though \mathbf{R} is available (in the Appendix), the computation time for (17) was prohibitive. An approximation of (17) is obtained by relative frequency interpretation. This approach first generates Gaussian random

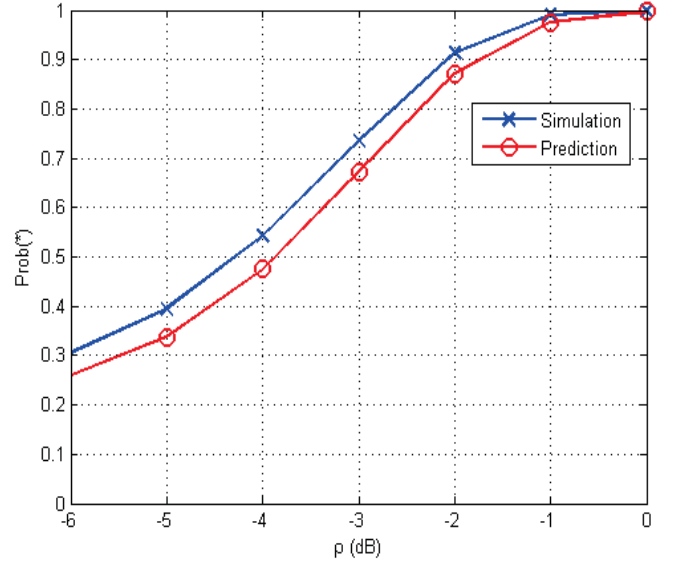


Fig. 3. Comparison of the experimental and predicted probability of obtaining the correct TDOA, $\text{Prob}(\ast)$, as a function of the signal-to-noise ratio ρ .

variables, representing Λ_* and $\boldsymbol{\gamma}$, that have \mathbf{R} as the co-variance matrix. It then counts the number of times that Λ_* is larger than all elements in $\boldsymbol{\gamma}$, over 50,000 trials. The percentage is close to the $\text{Prob}(\ast)$ of (17), and is the red curve in Fig. 3. The two plots are very close and for $\rho \geq 0$, $\text{Prob}(\ast) \approx 1$.

IV. CONCLUSIONS

In order to estimate the TDOA between two signals directly from their CS measurements, it is necessary to preserve the time shift relationship in the CS measurements. This is achieved by taking additional measurements of time shifted versions of the signals. A design of such a CS measurement system was presented. Results from simulation indicate the possibility of direct TDOA estimation without the need of reconstruction.

From (13), (10) and (11)

$$\Lambda_{i,j} = \langle \mathbf{A}(\mathbf{s}^{(i)} + \boldsymbol{\varphi}^{(i)}), \mathbf{A}(\mathbf{s}^{(j)} + \boldsymbol{\alpha}^{(j)}) \rangle \quad (19)$$

$$= \mathbf{s}^{(i)T} \mathbf{B} \mathbf{s}_D^{(j)} + \mathbf{s}^{(i)T} \mathbf{B} \boldsymbol{\alpha}^{(j)} + \boldsymbol{\varphi}^{(i)T} \mathbf{B} \mathbf{s}_D^{(j)} + \boldsymbol{\varphi}^{(i)T} \mathbf{B} \boldsymbol{\alpha}^{(j)} \quad (20)$$

where

$$\mathbf{B} = \mathbf{A}^T \mathbf{A}. \quad (21)$$

A direct computation shows that if \mathbf{A} ($M \times N$), with $M=N/2$ is the upper half of an $N \times N$ Hadamard matrix, \mathbf{B} has non-zero elements only at

$$\begin{aligned} b_{l,l} &= M, \quad l = 1, \dots, N \\ b_{l,l+M} &= M, \quad l = 1, \dots, M \\ b_{l+M,l} &= M, \quad l = 1, \dots, M. \end{aligned} \quad (22)$$

In the simulation example in Section III, $s(i)$, $\phi(i)$ and $\alpha(i)$ are all zero mean white Gaussian random variables. Hence for $i = j+D$, the expected value of (20) is

$$E\{\Lambda_*\} = NM\sigma_s^2 = \mu. \quad (23)$$

A straightforward but tedious evaluation then gives

$$\begin{aligned} \sigma_*^2 &= \text{Var}\{\Lambda_*\} = E\{\Lambda_*^2\} - \mu^2 \\ &= (NM^2 + 2M^3)(\sigma_s^2 + \sigma_\phi^2)^2 + 2NM^2\sigma_s^4. \end{aligned} \quad (24)$$

Similarly, for $i - j \neq D$,

$$E\{\Lambda_{i,j}\} = 0 \quad (25)$$

$$E\{\Lambda_{i,j}^2\} = \sigma^2 = (NM^2 + 2NM^3)(\sigma_s^2 + \sigma_\phi^2)^2. \quad (26)$$

For the specific case of $D = 3$ and $K = 4$ in Section III

$$\text{Cov}(\Lambda_{i,j}, \Lambda_{l,m}) = \begin{cases} \frac{\sigma^2}{2}, & i = j, l = m, \quad i \neq l \\ \sigma^2, & j = i+1, l = m+1, \quad j \neq l \\ 0, & \text{otherwise} \end{cases} \quad (27)$$

and

$$\text{Cov}(\Lambda_*, \Lambda_{i,j}) = 0, \quad i - j \neq D. \quad (28)$$

Now all the elements in the co-variance matrix are available

$$\mathbf{R} = E\left\{ \begin{bmatrix} \Lambda_* - \mu \\ \boldsymbol{\gamma} \end{bmatrix} \begin{bmatrix} \Lambda_* - \mu & \boldsymbol{\gamma} \end{bmatrix} \right\}. \quad (29)$$

- [1] L. Cheng, C. Wu and Y. Zhang, "Indoor robot localization based on wireless sensor networks," *IEEE Tran. Consumer Electronics*, Vol. 57, No. 3, pp.1099-1104, Aug, 2011.
- [2] A. Goetz, S. Zorn, R. Rose, G. Fisger, and R. Weigel, "A time difference of arrival system architecture for GSM mobile phone localization in search and rescue scenarios," *Workshop on Positioning Navigation and Communication (WPNC)*, pp. 24-27, 2011.
- [3] A. Ghelichi, K. Yelamarthi and A. Abdelgawad, "Target localization in wireless sensor network based on time difference of arrival," *IEEE International Midwest Symposium on Circuits and Systems (MWSCAS)*, pp.940-943, 2013.
- [4] Y.T. Chan and K.C. Ho, "A simple and efficient estimator for hyperbolic location," *IEEE Trans. Signal Processing*, Vol. 42, No. 8, pp.1905-1915, 1994.
- [5] C.H. Knapp and G.C. Carter, "The generalized correlation method for estimation of time delay," *IEEE Trans. Signal Processing*, Vol. 24, No. 4, pp.320-327, Aug. 1976.
- [6] E.J. Candes and M.B. Wakin, "An introduction to compressive sampling," *IEEE Signal Processing Magazine*, Vol. 25, No. 2, pp. 21-30, March 2008.
- [7] V. Cevher, A.C. Gurbuz, J.H. McClellan, and R. Chellappa, "Compressive wireless arrays for bearing estimation," *IEEE International Conf. on Acoustics, Speech and Signal Processing (ICASSP)*, pp. 2497-2500, 2008.
- [8] B. Miller, J. Goodman, K. Forsythe, J.Z. Sun, and V.K. Goyal, "A multi-sensor compressed sensing receiver: Performance bounds and simulated results," *Conference Record of the Asilomar Conf. on Signals, Systems and Computers*, pp.1571-1575, 2009.
- [9] B. Li, Y. Zou and Y. Zhu, "Direction estimation under compressive sensing framework: A review and experimental results," *IEEE International Conf. on Information and Automation (ICIA)*, pp.63-68, June 2011.
- [10] D. Yang, H. Lim, G.D. Peterson, and A. Fathy, "Compressive sensing TDOA for UWB positioning systems," *IEEE Radio and Wireless Symposium (RWS)*, pp.194-197, 2011.
- [11] K. Fyhn, M.F. Duarte and S.H. Jensen, "Compressive time delay estimation using interpolation," *IEEE Global Conf. on Signal and Information Theory*, Dec. 2013.
- [12] J. Yoo, C. Turnes, E.B. Nakumura, C.K. Lee, S. Becker, E.A. Sovero, M.B. Wakin, M.C. Grant, J. Romberg, A. Emami-Neyestanak, and E. Candes, "A compressed sensing parameter extraction platform for radar pulse signal acquisition," *IEEE Journal of Emerging and Selected Topics in Circuits and Systems*, Vol. 2, No. 3, pp. 626-638, Sept. 2012.